Feedback stabilizes propagation of synchronous spiking in cortical neural networks

Samat Moldakarimov[a,b], Maxim Bazhenov[a,c], and Terrence J. Sejnowski[a,b,d,1]

[a]Howard Hughes Medical Institute, Salk Institute for Biological Studies, La Jolla, CA 92037; [b]Institute for Neural Computation, University of California, San Diego, La Jolla, CA 92093; [c]Department of Cell Biology and Neuroscience, University of California, Riverside, CA 92521; and [d]Division of Biological Sciences, University of California, San Diego, La Jolla, CA 92093

Contributed by Terrence J. Sejnowski, January 15, 2015 (sent for review December 7, 2014; reviewed by Ernest Barreto)

Precisely timed action potentials related to stimuli and behavior have been observed in the cerebral cortex. However, information carried by the precise spike timing has to propagate through many cortical areas, and noise could disrupt millisecond precision during the transmission. Previous studies have demonstrated that only strong stimuli that evoke a large number of spikes with small dispersion of spike times can propagate through multilayer networks without degrading the temporal precision. Here we show that feedback projections can increase the number of spikes in spike volleys without degrading their temporal precision. Feedback also increased the range of spike volleys that can propagate through multilayer networks. Our work suggests that feedback projections could be responsible for the reliable propagation of information encoded in spike times through cortex, and thus could serve as an attentional mechanism to regulate the flow of information in the cortex. Feedback projections may also participate in generating spike synchronization that is engaged in cognitive behaviors by the same mechanisms described here for spike propagation.

neural coding | attention | cerebral cortex | synfire | spike timing

The firing rates of cortical neurons carry information about sensory inputs and motor actions (1). Precisely timed action potentials related to stimuli and behavior have also been observed in the cerebral cortex (2–4), and the mechanisms underlying precisely timed spike initiation have been studied in cortical neurons in vitro (5). However, the information carried by the precise timing of spikes would have to propagate through a hierarchy of cortical areas (6) and noise could disrupt millisecond precision during the transmission.

Previous modeling studies have demonstrated that synchronized volleys of spikes are essential for reliably driving the cortex by sparse thalamic inputs (7) and can indeed propagate through the layers of a feedforward network without compromising the temporal precision (8, 9). Furthermore, the temporal precision of a spike volley sharpens as it propagates through the network (10, 11). However, the results of these modeling studies suggest that only sufficiently strong stimuli that evoke spike volleys with a large number of spikes and a small dispersion of spike times would successfully propagate through the feedforward networks without degrading the temporal precision, whereas neural activities that are too weak or too dispersed will die out. This is a critical limitation on the propagation of synchronous spiking compared with the propagation of firing rates; stimuli evoking even low firing rate activity can successfully propagate through multilayer neural networks (12–14).

Here we show that when feedback connections are added to a multilayer feedforward model the propagation of synchronous spiking through the network layers is significantly enhanced without compromising temporal precision.

In our model with feedback projections, the state space of the model was divided into two areas: propagation and nonpropagation. In the propagation area all trajectories converged into an attractor state representing successful spike volley propagation; any spike volley starting anywhere inside this area successfully propagated through the network and reached the propagation attractor state with millisecond precision. Spike volleys starting outside the propagation area decayed after a few steps of transmission. The feedback changed the initial state of the spike volleys by moving them into the basin of the attractor for successful spike propagation. In addition, the feedback changed the position of the boundary separating propagation and nonpropagation areas, increasing the size of the basin of the propagation attractor.

Feedback projections are ubiquitous in the brain (15, 16), but little is known about what they contribute to information processing (17). The results presented here provide testable hypotheses for the functional role of the feedback projections in the brain.

Our model suggests that feedback projections could be responsible for allowing information encoded as spike times to propagate through cortical hierarchies, and therefore feedback projections could serve as an attentional mechanism to regulate the flow of information in the cortex. Feedback connections may also participate in generating spike-time synchronization among populations of neurons that are engaged in cognitive behaviors (18–20) by the same mechanisms described here for propagation of synchronized spikes through cortical areas.

Results

Feedforward Model. The feedforward model consisted of five layers of excitatory cells modeled using Hodgkin–Huxley (HH) formalism (*Materials and Methods*). In the feedforward model (Fig. 1*A*), a stimulus evoked spike volleys in the input layer of the

Significance

Feedback projections are ubiquitous in the brain, but little is known about what they contribute to information processing. The results presented here provide testable hypotheses for the functional role of the feedback projections in the brain. Our work suggests that feedback projections could be responsible for information encoded in spike times to reliably propagate through cortex, and thus could serve as an attentional mechanism to regulate the flow of information in the cortex. Our work also suggests that feedback projections may also be critically involved in organizing neural populations involved in cognitive functions by generating and sharpening spike-time synchronization among populations of neurons. Thus, feedback projections could be key to understanding how the cortex is globally organized.

Author contributions: S.M., M.B., and T.J.S. designed research; S.M. performed research; S.M. analyzed data; and S.M., M.B., and T.J.S. wrote the paper.

Reviewers included: E.B., George Mason University.

The authors declare no conflict of interest.

[1]To whom correspondence should be addressed. Email: terry@salk.edu.

This article contains supporting information online at www.pnas.org/lookup/suppl/doi:10.1073/pnas.1500643112/-/DCSupplemental.

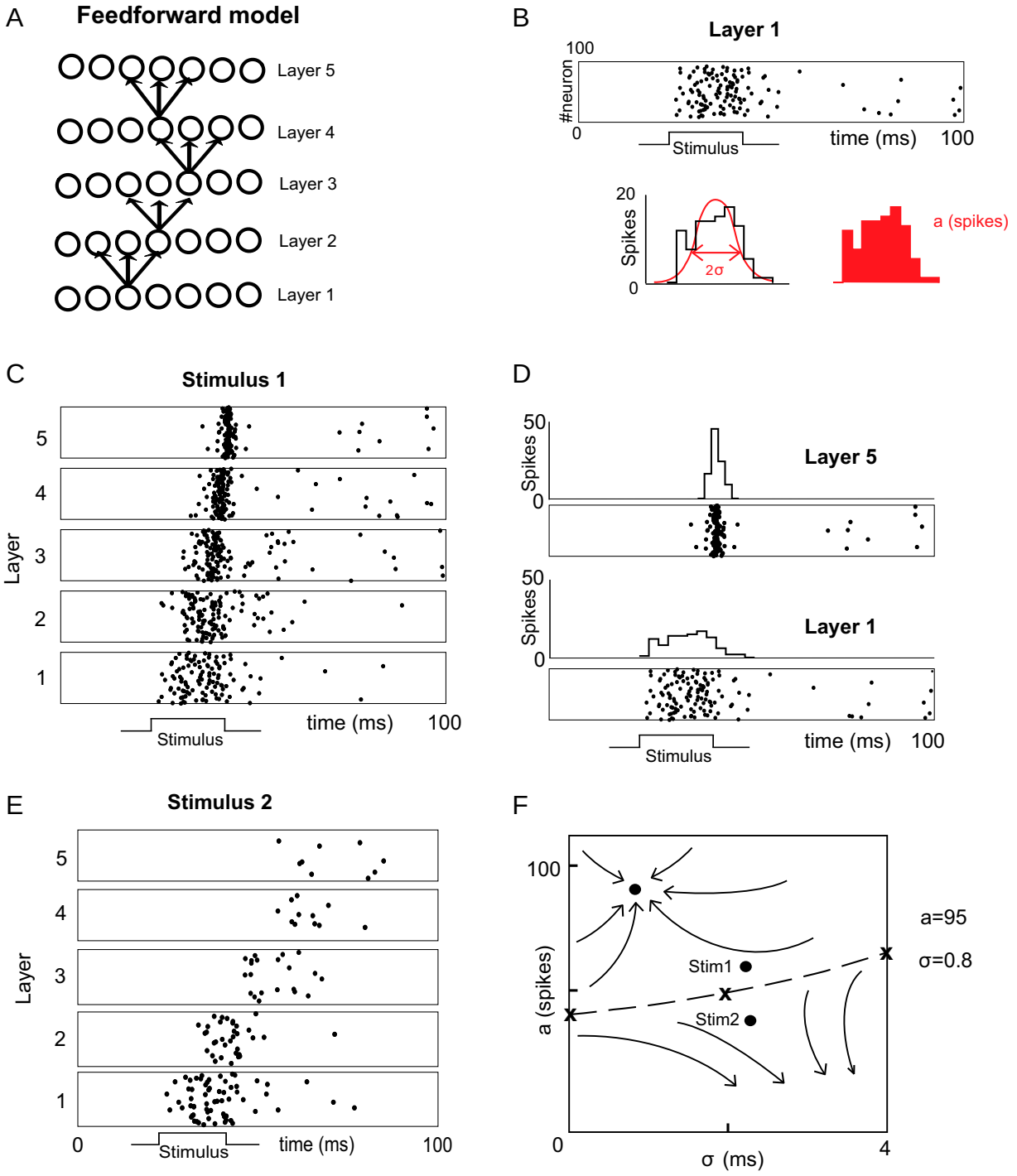

Fig. 1. Demonstration of a propagating volley in a feedforward network model. (*A*) Feedforward network. (*B*) (*Upper*) Stimulus-evoked spike volley in layer 1 of the network. (*Lower*) Estimation of the number of spikes (**a**) and the width of the volley (**σ**). (*C*) Propagation of stimulus 1 (number of spikes **a** = 69, and dispersion **σ** = 2.2) through the feedforward network. (*D*) Spike histograms in layer 1 and layer 5, in response to stimulus 1. (*E*) Propagation of a weaker stimulus 2 (**a** = 37, **σ** = 2.2) through the feedforward network. (*F*) Attractor state in the state space (**a** = 95, **σ** = 0.8). The propagation (upper) and nonpropagation (lower) areas are separated by separatrix (dashed line). Stim1 and Stim2 are locations of activity states in layer 1 evoked by stimulus 1 and stimulus 2, respectively.

network (layer 1) that were characterized by two parameters: number of spikes in the volley, **a**, and temporal dispersion characterized by SD of the underlying spike density, **σ** (Fig. 1*B*).

Our goal was to predict when activity could and could not propagate through the network based on activity of neurons in layer 1.

Stimulus 1 evoked a spike volley in layer 1 with a high number of spikes (**a** = 69), which successfully propagated through the network (Fig. 1*C*). The spike timing dispersion narrowed and the spikes tended to synchronize as the activity propagated through the network (Fig. 1*D*). The convergence of spike times in the feedforward network was due to the shared inputs (10, 11). Neurons that shared a large enough pool of synchronized input cells tended to align their action potentials, which resulted in synchrony increasing from lower to higher layers

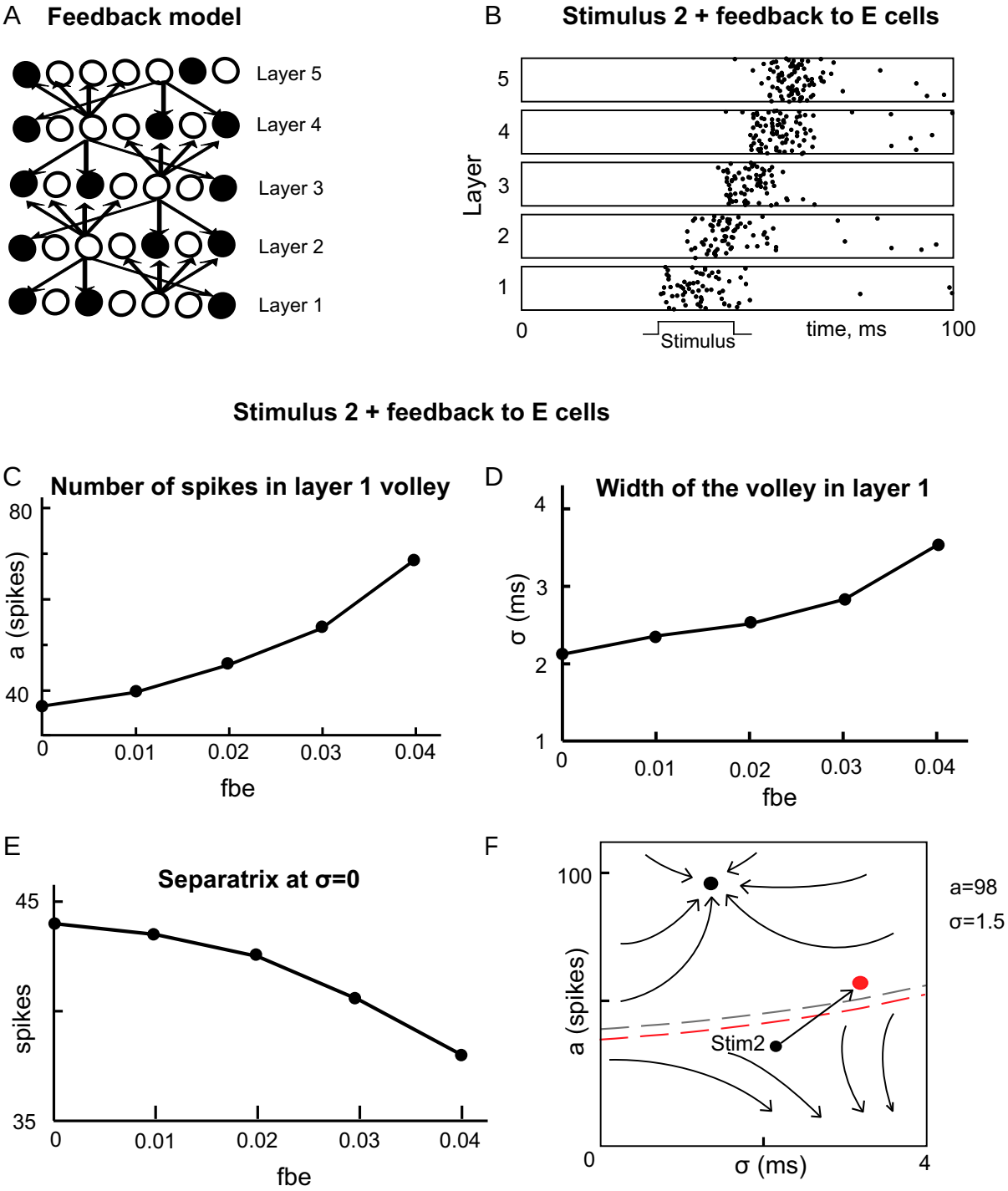

Fig. 2. Demonstration of a propagating volley in a network model with feedback connections. (*A*) Feedback network. (*B*) Propagation of stimulus 2 (**a** = 37, **σ** = 2.2) through the network with feedback to E cells. (*C*) Number of spikes in the pulse packet as the function of the strength of the feedback connections to excitatory cells (fbe). (*D*) Width of the spike volley (**σ**) as the function of the strength of feedback connections to excitatory cells (fbe). (*E*) Location of the separatrix as the function of the feedback strength. (*F*) Attractor state in the state space (**a** = 98, **σ** = 1.5). The new separatrix (red dashed line) separates stable (upper) and unstable (lower) areas. The black dashed line represents the initial separatrix for the feedforward model. Both the initial state (**a** and **σ**) and the separatrix changed due to the feedback (fbe = 0.03).

owing to synchronized neurons in each layer activating neurons in the next layer more effectively.

Stimulus 2 evoked fewer spikes in layer 1 (**a** = 37) than stimulus 1, and the spikes could not propagate in the feedforward model (Fig. 1*E*).

Propagation of a spike volley in the feedforward model (Fig. 1*C*) or failure of propagation (Fig. 1*E*) depended on both features of the spike volley in layer 1: the number of spikes in the volley and the dispersion of spike times in layer 1 (Fig. 1*F*). Our analysis showed that separatrix divided the state place into two regions: Stimuli that evoked activity in layer 1 represented by the states above the separatrix propagated through the network and converged to an attractor, but stimuli that evoked activity represented by the states below the separatrix could not propagate

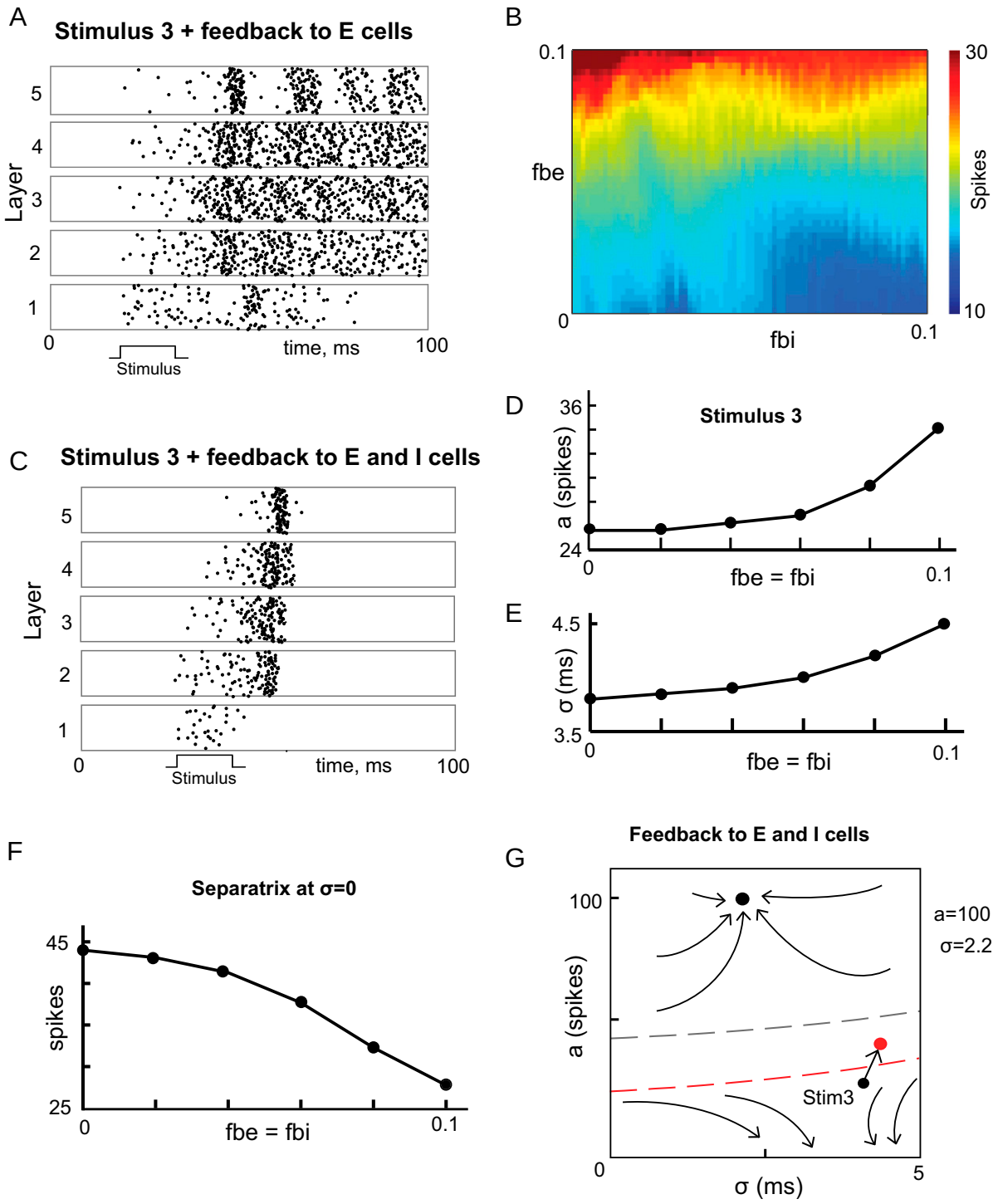

Fig. 3. Differential effects of feedback to excitatory and inhibitory neurons. (*A*) Propagation of stimulus 3 (**a** = 26, **σ** = 3.5) through the network with feedback to excitatory cells (fbe = 0.08). (*B*) Number of spike in a volley depended on the strength of feedback to the excitatory (fbe) and inhibitory (fbi) cells. (*C*) Propagation of stimulus 3 through the network with feedback to both excitatory and inhibitory cells (fbe = fbi = 0.1). (*D*) Number of spikes in the spike volley as the function of the feedback strengths (fbe = fbi). (*E*) Width of the volley as the function of the feedback strength (fbe = fbi). (*F*) Location of the separatrix as the function of the feedback strengths. (*G*) Attractor state (**a** = 100, **σ** = 2.2). The propagation (upper) and nonpropagation (lower) areas are separated by the new separatrix (red dashed line). The black dashed line represents the initial separatrix for the feedforward model, the same black dashed line as in Fig. 2*F*. Both the state and the separatrix shifted due to the feedback (fbe = fbi = 0.1).

(Fig. 1*F*). The separatrix, which determined the boundary between two outcomes, did not depend on stimuli and therefore did not change during simulations.

Feedback Model with Excitatory Cells. Adding feedback from the excitatory neurons back to the excitatory neurons in the previous layer (Fig. 2*A*) resulted in stimulus 2, which could not propagate

in the feedforward model to successfully propagate through the network (Fig. 2*B*).

In the network with feedback, the initial state of the spike volley depended both on the stimulus and the feedback. Indeed, the feedback to the excitatory cells increased both the number of spikes (Fig. 2*C*) and the width of the spike volley (Fig. 2*D*) in layer 1. Because of these changes, the state of the layer 1 spike volley (initial state) in response to the same stimulus 2 as in Fig. 1 moved up and to the right in the state space (Fig. 2*F*). As a result, the initial state of the spike volley was now in the propagation region above the separatrix, which allowed a stimulus that could not previously propagate in the pure feedforward model to propagate through the feedback network (Fig. 2*B*).

The feedback to excitatory cells also slightly lowered the separatrix (Fig. 2*E*), which resulted in a moderate increase of the basin of the propagation attraction (Fig. 2*F*) (see also below and Fig. 3, where the shift of the separatrix is much more significant in the model with feedback connections to both excitatory and inhibitory cells). The feedback to excitatory cells lowered the separatrix and expanded the basin of the propagation attractor through amplification of the neural activity in all layers of the network, because the feedback was present between all pairs of the adjacent layers.

However, the feedback projections to the excitatory neurons enhanced spike propagation through the network only for stimuli with initial states close to the separatrix (Fig. 2*F*). For new stimulus 3, which was selected to be weaker than previously applied stimulus 2, and therefore had an initial state that was far below the separatrix, the strong feedback projections led to artifacts, such as oscillatory activity in the higher layers (Fig. 3*A*). This occurred because the strong feedback inputs into the excitatory neurons not only added spikes to the volley but also caused activity to reverberate between layers (Fig. 3*A*).

Feedback Model with Excitatory and Inhibitory Cells. To overcome the aforementioned limitations of the feedback model consisting of the excitatory cells alone, we included into the feedback model both the excitatory and inhibitory cells. Both feedforward and feedback connections originated from the excitatory cells in each layer, but the feedforward connections targeted the excitatory cells, whereas the feedback connections targeted both the excitatory and inhibitory cells.

We explored the effect of the feedbacks on the number of spikes in the volley. Feedback to solely the excitatory cells increased number of spikes in the volleys, whereas feedback to the inhibitory cells alone decreased the number of spikes (Fig. 3*B*). Because experimental data suggest that the feedback to the excitatory cells and feedback to the inhibitory cells are not independent from each other (21), we have chosen the feedback to the excitatory and inhibitory cells to be similar to explore how the change of feedback affects spike propagation. The similar feedback to both excitatory and inhibitory neurons enhanced spike propagation for stimulus 3 (Fig. 3*C*). The feedback to the excitatory neurons increased the number of spikes (Fig. 3*D*) and the width of the volley (Fig. 3*E*), but the feedback to the inhibitory neurons prevented the width of the volley from growing uncontrollably, which eliminated the reverberation of activity and oscillatory artifacts (compare Fig. 3 *A* and *C*).

Importantly, feedback to both excitatory and inhibitory neurons lowered the separatrix in the state space by 40%, which significantly increased the basin of attraction of a propagating state compared with the model with feedback to excitatory cells alone (Fig. 3*F*). This increase of the basin of propagation attractor was due to much stronger feedbacks to the excitatory cells, which were balanced by strong feedbacks to the inhibitory cells. All these effects combined—changes of the initial state and the separatrix—resulted in the initial state of stimulus 3 moving to the basin of propagation attractor (Fig. 3*G*).

We conclude that feedback to both the excitatory and inhibitory cells can significantly increase the range of stimuli that could propagate through the network.

Discussion

In purely feedforward models of cortical networks only strong stimuli can successfully propagate through the hierarchy of cortical layers without degradation of temporal precision, and neural activities evoked by weak stimuli die out (8–11). Here we have shown that feedback connections in a cortical network model can enhance propagation of synchronous spiking through the neural networks while preserving temporal precision of spiking. This enhancement was partly due to the feedback inputs increasing the number of spikes in the volleys. The location of the separatrix bounding the basin of propagation attractor in the state space was another critical parameter that determined the conditions for propagation of synchronous spiking in the network. The feedback both increased the number of spikes in the spike volleys and moved the separatrix downward, which expanded the basin of the attraction. These two effects of the feedback increased the range of stimuli able to propagate through the network. The feedback inputs into both the excitatory and inhibitory neurons allowed much stronger enhancement of synchronous spike propagation compared with the feedback to excitatory neurons alone.

Our work suggests that feedback projections can strongly modulate the propagation of spiking activity, and therefore could serve as an attentional mechanism to regulate the flow of information in the cortex (22). This attentional effect of corticocortical feedback projections could be based on neuromodulation that can regulate both the excitatory and inhibitory synapses in cortical neurons (23). In addition, feedback may also differentially affect different types of cortical neurons (24), in particular inhibitory neurons, which are important for regulating the timing of spikes in cortical networks (25). The mechanisms of feedback modulation may also regulate the gain of neurons, which also affects the balance between cortical excitation and inhibition.

Spike-time synchronization may organize populations of neurons that are engaged in cognitive behaviors (18–20). The contribution of the recurrent cortical connections in the generation of synchronized neural populations has been previously emphasized (26). However, feedback connections may also play a critical role in generation of spike synchronization that engaged in cognitive behaviors by the same mechanisms described here for propagation of synchronized spikes through cortical areas. The widespread diffuse nature of feedback projections could facilitate synchronization of neural populations that cannot be synchronized by long-range lateral connections.

Feedback inputs have also been used to implement predictive coding (27). According to this approach, cortical networks learn the statistical regularities of the natural stimuli and reduce redundancy by removing the predictable parts of the input to focus on what is different. This coding scheme is compatible with our model but would require much more precise targeting for the feedback projections to achieve predictive coding capability.

Synfire chains can be considered a special case of polychronous chains (28). In polychronous chains, spike times in an ensemble of neurons are time-locked but not synchronized. Because the propagation in polychronous chains also depends on the coincidence of spike arrival times, feedback projections should enhance propagation in polychronous chains through the same mechanisms described in this study.

In conclusion, feedback projections are ubiquitous in the cortex (15, 16), but little is known about how they contribute to information processing (17). The results presented here provide testable hypotheses for the function of the feedback projections in the brain as a mechanism of enhancing robustness of the

transmission of information encoded in spike times. Selective manipulation of the feedback pathways has been a difficult problem. New techniques using optogenetics could be used to test these predictions, such as expressing halorhodopsin or channelrhodopsin in feedback neurons and stimulating with light to selectively reduce or enhance feedback activity with temporal precision (29).

Materials and Methods

Feedforward Model. The feedforward model consisted of five layers of spiking neurons with 100 excitatory HH model neurons in each layer (30) (Fig. 1*A*). Neurons in each layer projected to all neurons in the next layer. There were no recurrent connections within layers.

Feedback Model. The feedback model also had five layers of spiking neurons. Each layer contained 100 excitatory and 25 inhibitory conductance-based HH neurons. Excitatory cells projected back nonselectively to all excitatory cells, but not the inhibitory cells (in simulations for Figs. 2 and 3*A*) or to both the excitatory and inhibitory cells (in simulations for Fig. 3 *B*–*G*). The recurrent connections included connections from every inhibitory cell to all excitatory cells in each layer.

HH Neuron Model. Conductance-based HH equations were used to model neurons in the spiking neural network model. By using a conductance-based HH model, we reproduced previous results obtained by using a leaky integrate-and-fire (LIF) model (10), which allowed us to conclude that the type of spiking neuron model is not critical for the observed network behavior. Model parameters were chosen to fit the spike properties of regular spiking pyramidal neurons and fast-spiking interneurons (31).

Stimuli. We applied three different stimuli to the model by changing the number of spikes in the spike volley and dispersion among spike times. This was done by varying the number of randomly activated neurons in layer 1 and by changing the amount of injected noisy currents into neurons in all layers [stimulus 1 ($\mathbf{a} = 69$, $\boldsymbol{\sigma} = 2.2$), stimulus 2 ($\mathbf{a} = 37$, $\boldsymbol{\sigma} = 2.2$), and stimulus 3 ($\mathbf{a} = 26$, $\boldsymbol{\sigma} = 3.5$)].

Noise. In the model, noisy excitatory currents resulted in spontaneous activity on average 5 Hz. Noise also prevented neurons from becoming fully synchronized, but surprisingly noise did not lead to deterioration of the propagated activity. In addition, we controlled the level of noise so that it was not strong enough to switch the network's behavior from synfire chain to rate propagation, as in ref. 12.

Separatrix. We drew the boundary between propagation and nonpropagation regimes (separatrix) by testing the state space of the system ($\mathbf{a}$, $\boldsymbol{\sigma}$) to determine which initial conditions lead to propagation through the network and which ones do not. Thus, we varied systematically the number of spikes in the spike volley for three fixed dispersions of spike time distribution $\boldsymbol{\sigma} = 0$, $\boldsymbol{\sigma} = 2$, and $\boldsymbol{\sigma} = 4$. At each point we assessed the boundary with precision of one to two spikes. Then we approximated the boundary in the state space by a smooth line.

State-Space Analysis. We have selected the state-space variables to be consistent with the previous analysis of the feedforward model and to be able to compare the feedforward and feedback models. The amplitude of the stimulus and its duration could be also used as state-space variables to explore conditions under which stimuli can and cannot propagate. The main conclusions may not differ qualitatively, except with stimulus-centric coordinates we could only assess the separatrix, and to understand the dynamics of neural activity and discuss attractor states we need to know the activity state in each layer.

ACKNOWLEDGMENTS. This work was supported by the Howard Hughes Medical Institute, Office of Naval Research Multidisciplinary University Initiative Grants N00014100072 and N000141310672, and National Institutes of Health Grants R01EB009282, R01DC006306, R01DC012943, and R01NS060870.

1. Shadlen MN, Newsome WT (1994) Noise, neural codes and cortical organization. *Curr Opin Neurobiol* 4(4):569–579.
2. Abeles M, Bergman H, Margalit E, Vaadia E (1993) Spatiotemporal firing patterns in the frontal cortex of behaving monkeys. *J Neurophysiol* 70(4):1629–1638.
3. Bair W, Koch C (1996) Temporal precision of spike trains in extrastriate cortex of the behaving macaque monkey. *Neural Comput* 8(6):1185–1202.
4. Haider B, et al. (2010) Synaptic and network mechanisms of sparse and reliable visual cortical activity during nonclassical receptive field stimulation. *Neuron* 65(1): 107–121.
5. Mainen ZF, Sejnowski TJ (1995) Reliability of spike timing in neocortical neurons. *Science* 268(5216):1503–1506.
6. Felleman DJ, Van Essen DC (1991) Distributed hierarchical processing in the primate cerebral cortex. *Cereb Cortex* 1(1):1–47.
7. Wang HP, Spencer D, Fellous JM, Sejnowski TJ (2010) Synchrony of thalamocortical inputs maximizes cortical reliability. *Science* 328(5974):106–109.
8. Kumar A, Rotter S, Aertsen A (2008) Conditions for propagating synchronous spiking and asynchronous firing rates in a cortical network model. *J Neurosci* 28(20):5268–5280.
9. Kumar A, Rotter S, Aertsen A (2010) Spiking activity propagation in neuronal networks: Reconciling different perspectives on neural coding. *Nat Rev Neurosci* 11(9): 615–627.
10. Diesmann M, Gewaltig M-O, Aertsen A (1999) Stable propagation of synchronous spiking in cortical neural networks. *Nature* 402(6761):529–533.
11. Reyes AD (2003) Synchrony-dependent propagation of firing rate in iteratively constructed networks in vitro. *Nat Neurosci* 6(6):593–599.
12. van Rossum MC, Turrigiano GG, Nelson SB (2002) Fast propagation of firing rates through layered networks of noisy neurons. *J Neurosci* 22(5):1956–1966.
13. Litvak V, Sompolinsky H, Segev I, Abeles M (2003) On the transmission of rate code in long feedforward networks with excitatory-inhibitory balance. *J Neurosci* 23(7): 3006–3015.
14. Vogels TP, Abbott LF (2005) Signal propagation and logic gating in networks of integrate-and-fire neurons. *J Neurosci* 25(46):10786–10795.
15. Salin P-A, Bullier J (1995) Corticocortical connections in the visual system: Structure and function. *Physiol Rev* 75(1):107–154.
16. Callaway EM (2004) Feedforward, feedback and inhibitory connections in primate visual cortex. *Neural Netw* 17(5-6):625–632.
17. Bullier J (2005) What is fed back? *23 Problems in Systems Neuroscience*, eds Van Hemmen JL, Sejnowski TJ (Oxford Univ Press, New York), pp 103–132.
18. Fries P, Reynolds JH, Rorie AE, Desimone R (2001) Modulation of oscillatory neuronal synchronization by selective visual attention. *Science* 291(5508):1560–1563.
19. Baldauf D, Desimone R (2014) Neural mechanisms of object-based attention. *Science* 344(6182):424–427.
20. Yamamoto J, Suh J, Takeuchi D, Tonegawa S (2014) Successful execution of working memory linked to synchronized high-frequency gamma oscillations. *Cell* 157(4):845–857.
21. Haider B, Duque A, Hasenstaub AR, McCormick DA (2006) Neocortical network activity in vivo is generated through a dynamic balance of excitation and inhibition. *J Neurosci* 26(17):4535–4545.
22. Salinas E, Sejnowski TJ (2001) Correlated neuronal activity and the flow of neural information. *Nat Rev Neurosci* 2(8):539–550.
23. Disney AA, Aoki C, Hawken MJ (2007) Gain modulation by nicotine in macaque v1. *Neuron* 56(4):701–713.
24. Mitchell JF, Sundberg KA, Reynolds JH (2007) Differential attention-dependent response modulation across cell classes in macaque visual area V4. *Neuron* 55(1): 131–141.
25. Tiesinga P, Fellous JM, Sejnowski TJ (2008) Regulation of spike timing in visual cortical circuits. *Nat Rev Neurosci* 9(2):97–107.
26. Buzsáki G, Wang XJ (2012) Mechanisms of gamma oscillations. *Annu Rev Neurosci* 35:203–225.
27. Rao RP, Ballard DH (1999) Predictive coding in the visual cortex: A functional interpretation of some extra-classical receptive-field effects. *Nat Neurosci* 2(1):79–87.
28. Izhikevich EM (2006) Polychronization: Computation with spikes. *Neural Comput* 18(2):245–282.
29. Zhang F, et al. (2011) The microbial opsin family of optogenetic tools. *Cell* 147(7): 1446–1457.
30. Dayan P, Abbott LF (2001) *Theoretical Neuroscience* (MIT Press, Cambridge, MA).
31. McCormick DA, Huguenard JR (1992) A model of the electrophysiological properties of thalamocortical relay neurons. *J Neurophysiol* 68(4):1384–1400.

Supporting Information

Moldakarimov et al. 10.1073/pnas.1500643112

SI Materials and Methods

Feedforward Model. The feedforward model consisted of five layers of spiking neurons with 100 excitatory HH model neurons in each layer (1) (Fig. 1*A*). Neurons in each layer projected to all neurons in the next layer. There were no recurrent connections within layers.

Feedback Model. The feedback model had five layers of spiking neurons. Each layer contained 100 excitatory and 25 inhibitory conductance-based HH neurons. Excitatory cells projected back to all of the excitatory cells, but not the inhibitory cells (in simulations for Fig. 2 and Fig. 3*A*) or all excitatory and inhibitory cells (in simulations for Fig. 3 *B*–*G*). The recurrent connections included connections from every inhibitory cell to all excitatory cells in each layer.

HH Neuron Model. Conductance-based HH equations were used to model neurons in the spiking neural network model. We first reproduced previous results (2), which used an LIF model, by using a conductance-based HH model, which allowed us to conclude that the type of spiking neuron model is not critical for the observed network behavior.

Excitatory neurons.

$$C\frac{dV_e}{dt} = I_{exte} - I_{mem}(V_e, m_e, n_e, h_e) - I_{syne} - I_{AHP}$$

$$I_{mem} = g_{Le}\cdot(V - V_L) + g_K\cdot n^4\cdot(V - V_K) + g_{Na}\cdot m_\infty^3\cdot h\cdot(V - V_{Na})$$

$$I_{AHP} = g_{AHP}\cdot\frac{[Ca]}{1+[Ca]}\cdot(V_e - V_K)$$

$$m_\infty(V) = \frac{\alpha_m(V)}{\alpha_m(V)+\beta_m(V)}$$

$$\alpha_m(V) = \frac{0.1\cdot(V+30)}{1-e^{-0.1\cdot(V+30)}}$$

$$\beta_m(V) = 4\cdot e^{-(V+55)/18}$$

$$\frac{dn}{dt} = 3\cdot(\alpha_n(V)\cdot(1-n) - \beta_n(V)\cdot n)$$

$$\alpha_n(V) = \frac{0.01\cdot(V+34)}{1-e^{-0.1\cdot(V+34)}}$$

$$\beta_n(V) = 0.125\cdot e^{-(V+44)/80}$$

$$\frac{dh}{dt} = 3\cdot(\alpha_h(V)\cdot(1-h) - \beta_h(V)\cdot h)$$

$$\alpha_h(V) = 0.07\cdot e^{-(V+44)/20}$$

$$\beta_h(V) = \frac{1}{1-e^{-0.01\cdot(V+14)}}$$

$$\frac{d[Ca]}{dt} = \frac{-0.002\cdot g_{Ca}\cdot(V_e - V_{Ca})}{1+e^{-(V_e+25)/2.5}} - [Ca]/\tau_{Ca},$$

where V_e is membrane potential of an excitatory neuron; m, h, and n are the gating variables of voltage-gated sodium and potassium channels; g_L is maximum conductance of the leak current; g_{Na} is maximum conductance of sodium current; g_K is maximum conductance of potassium current; V_L is reversal potential of the leak current; V_{Na} is reversal potential for sodium currents; V_K is reversal potential for potassium currents; and g_{AHP} is the maximum conductance of the calcium-dependent potassium current.

Model parameters were chosen to fit the spike properties of regular spiking pyramidal neurons (3):

$g_{Le} = 0.05,\ g_{Na} = 100,\ g_K = 40,\ g_{Ca} = 0.9,\ V_L = -65,\ V_{Na} = 55,\ V_K = -80,\ V_{Ca} = 120,\ \tau_{Ca} = 100.$

Inhibitory neurons. The HH equation for the membrane potential of the inhibitory neurons was

$$C\frac{dV_i}{dt} = I_{exti} - I_{mem}(V_i, m_i, n_i, h_i) - I_{syni},$$

where V_i is membrane potential of an inhibitory neuron and m, h, and n are the gating variables for the ionic currents. The dynamics of the gating variables m, h, and n were the same as for the excitatory neuron. The differences between them were, first, that the inhibitory neurons lacked the I_{AHP} current and, second, the inhibitory interneurons membrane time constants were shorter. Because the membrane time scale τ_{mem} is related to the membrane leak conductance g_L by $\tau_{mem}\sim 1/g_L$, in the inhibitory cells $g_{Li} = 0.1$ and in the excitatory cells $g_{Le} = 0.05$. Thus, the dynamics of the inhibitory cells was faster compared with the excitatory cells.

Synaptic models. Models for the excitatory AMPA receptor and inhibitory GABA receptor were used to simulate synaptic interactions:

$$\frac{ds_e}{dt} = \frac{\left(\frac{1-s_e}{1+e^{-(V_e+20)/4}} - s_e\right)}{\tau_{AMPA}}$$

$$\frac{ds_i}{dt} = \frac{\left(\frac{1-s_i}{1+e^{-(V_i+20)/4}} - s_i\right)}{\tau_{GABAa}},$$

where s_e is a synaptic gating variable of AMPA current, s_i is a synaptic gating variable of $GABA_A$ current, $\tau_{AMPA} = 2$, and $\tau_{GABAa} = 7$.

Synaptic currents. The synaptic currents to an excitatory neuron were

$$I_{exc} = I_{ee} + I_{ei} = \frac{1}{N_e}\sum_e (s_e\cdot f_e)\cdot(V_e - V_{ee}) + \frac{1}{N_i}\sum_i (s_i\cdot f_i)\cdot(V_e - V_{ei})$$

and the synaptic current to an inhibitory neuron

$$I_{inh} = \frac{1}{N_e}\sum_e (s_e\cdot f_e)\cdot(V_i - V_{ie}),$$

where V_e is membrane potential of an excitatory neuron, V_i is membrane potential of an inhibitory neuron, s_e is synaptic gating

variables of AMPA currents, s_i is synaptic gating variable of $GABA_A$ current, f_e and f_i are synaptic depression factors, and $V_{ei} = 80$, $V_{ee} = 0$, and $V_{ei} = 0$.

Stimuli. We applied different stimuli to the model by changing the number of spikes in the spike volley and dispersion among spike times. This was done by varying the number of randomly activated neurons in layer 1 and by changing the amount of injected noisy currents into neurons in all layers [stimulus 1 ($\mathbf{a} = 69$, $\boldsymbol{\sigma} = 2.2$), stimulus 2 ($\mathbf{a} = 37$, $\boldsymbol{\sigma} = 2.2$), and stimulus 3 ($\mathbf{a} = 26$, $\boldsymbol{\sigma} = 3.5$)].

Noise. In the model, noisy excitatory currents resulted in spontaneous activity on average 5 Hz. Noise also prevented neurons to become fully synchronized, but surprisingly noise did not lead to deterioration of the propagated activity. In addition, we controlled the level of noise so it would not be strong enough to switch the network's behavior from synfire chain to rate propagation, as in ref. 4.

Separatrix. We drew the separatrix by testing the state space of the system ($\mathbf{a}$, $\boldsymbol{\sigma}$) to determine which initial conditions lead to propagation through the network and which ones do not. Thus, we varied systematically the number of spikes in the spike volley for fixed dispersions of spike time distribution $\boldsymbol{\sigma} = 0$, $\boldsymbol{\sigma} = 2$, and $\boldsymbol{\sigma} = 4$. At each point we assessed the boundary with precision of one to two spikes. Then we approximated the boundary in the state space by a smooth line.

State-Space Analysis. We have selected the state-space variables to be consistent with the previous analysis of the feedforward model, and to be able to compare the feedforward and feedback models. Amplitude of the stimulus and its duration could be also used as state-space variables to explore conditions under which stimuli can and cannot propagate. The main conclusions may not differ qualitatively, except with stimulus-centric coordinates we could only assess the separatrix, and to understand the dynamics of neural activity and discuss attractor states we need to know activity state in each layer.

1. Dayan P, Abbott LF (2001) *Theoretical Neuroscience* (MIT Press, Cambridge, MA).
2. Diesmann M, Gewaltig M-O, Aertsen A (1999) Stable propagation of synchronous spiking in cortical neural networks. *Nature* 402(6761):529–533.
3. McCormick DA, Huguenard JR (1992) A model of the electrophysiological properties of thalamocortical relay neurons. *J Neurophysiol* 68(4):1384–1400.
4. van Rossum MC, Turrigiano GG, Nelson SB (2002) Fast propagation of firing rates through layered networks of noisy neurons. *J Neurosci* 22(5):1956–1966.